A LEED analysis of the clean surfaces of α-Fe_2O_3(0001) and α-Cr_2O_3(0001) bulk single crystals

2009 J. Phys.: Condens. Matter 21 134010

(http://iopscience.iop.org/0953-8984/21/13/134010)

J. Phys.: Condens. Matter **21** (2009) 134010 (8pp) doi:10.1088/0953-8984/21/13/134010

A LEED analysis of the clean surfaces of α-$Fe_2O_3(0001)$ and α-$Cr_2O_3(0001)$ bulk single crystals

Maike Lübbe and Wolfgang Moritz

Department of Earth and Environmental Sciences, Section Crystallography,
Ludwig-Maximilians-Universität München, Theresienstraße 41, 80333 Munich, Germany

E-mail: maike.luebbe@lrz.uni-muenchen.de

Received 10 November 2008, in final form 2 February 2009
Published 12 March 2009
Online at stacks.iop.org/JPhysCM/21/134010

Abstract

We analyzed the (0001) surface structures of hematite and chromia bulk single crystals by low energy electron diffraction (LEED). The hematite crystal was annealed in an O_2 atmosphere, $p_{O_2} \approx 3 \times 10^{-8}$ mbar, for several hours. The chromia crystal was sputtered with Ar^+ ions, $E = 1$ keV, and afterward heated up to 900 °C for 5 min under ultra-high-vacuum (UHV) conditions. $I(V)$-curve data sets of 12 symmetrically independent diffraction spots were measured at room temperature in the energy range $E = 150$–500 eV. Charging effects hindered measurements at lower energies. Our analysis of the hematite single crystal surface indicates that it is terminated by a single iron layer which is occupied at ≈50%. Relaxation effects along the c-axis are quite large and involve several iron double layers. For the chromia surface the results indicate that termination with a single Cr seems not to hold. Most probably the surface is terminated by two partially occupied Cr sites or chromyl groups. Relaxations in deeper layers are small in contrast to α-$Fe_2O_3(0001)$.

(Some figures in this article are in colour only in the electronic version)

1. Introduction

Metal oxides are of great technological and scientific interest, not only due to their catalytic activities but also because they play an important role in the development of novel electronic devices. Nevertheless, the surface structure of many metal oxides, which is a crucial point in understanding processes at or near the surface, has not been resolved unambiguously up to now. Among these are the transition metal oxides α-Fe_2O_3 (hematite) and α-Cr_2O_3 (chromia) which are both corundum-type oxides.

Hematite is interesting for chemical and technological applications. It is also an important oxide in studies of magnetism and was recently included in DMS (diluted magnetic semiconductor) research (Chambers 2006). Experimental investigations including LEED (Ketteler *et al* 2001) and STM studies (Chambers and Yi 1999, Thevuthasan *et al* 1999, Shaikhutdinov and Weiss 1999, Lemire *et al* 2005) have been carried out on hematite thin films. X-ray diffraction (XRD) measurement was performed with a bulk single crystal exposed to air or near a water-saturated He atmosphere (Trainor *et al* 2004). Most results are not consistent with each other, claiming different terminations for similar preparation conditions or terminations not depending on preparation conditions at all, while others find strong dependence. But all results support the theoretical prediction of significant interlayer relaxations.

Theory predicts a single iron termination (Fe–O_3–Fe_2–···) to be stable at low and intermediate oxygen partial pressures. The topmost Fe layer relaxes strongly towards the underlying O_3 layer and the interlayer distance between the two Fe atoms in the first double iron layer decreases significantly (Wang *et al* 1998, Bergermayer *et al* 2004). Furthermore 50% iron vacancies are said to be present in the top Fe layer (Rohrbach *et al* 2004). For higher oxygen pressures a ferryl termination (O=Fe–O_3–Fe_2–···) and then the oxygen termination (O_3–Fe_2–···) become the most stable ones (Bergermayer *et al* 2004, Rohrbach *et al* 2004). A combined density functional theory (DFT) and crystal truncation rod (CTR) diffraction study of a α-$Fe_3O_4(0001)$ surface in a water-saturated atmosphere suggests that the hydrated surface is terminated by mixed domains of a hydroxylated single iron termination ($(HO)_3$–Fe–H_3O_3–Fe_2–···)

and a hydroxylated oxygen termination ($(HO)_3$–Fe_2–$\cdots$) (Trainor *et al* 2004). The results we report here refer to a surface prepared in an ultra-high-vacuum (UHV) and hydroxylation seems unlikely. Therefore we did not consider hydroxylated models in the LEED $I(V)$ analysis.

The results of the various experiments are contradictory. A single iron termination is found despite highly oxidizing conditions during preparation (Chambers and Yi 1999, Thevuthasan *et al* 1999) as well as for low oxygen partial pressures only and then switching to an oxygen termination at higher pressures (Shaikhutdinov and Weiss 1999). The coexistence of a single iron and an oxygen termination after oxidation at 1100 K and 10^{-3} mbar oxygen pressure (Wang *et al* 1998) and a single iron termination with a ferryl termination after preparation at 1050 K and 10^{-3} to 1 mbar oxygen pressure (Lemire *et al* 2005) is also reported. Oxygen terminations (O_3–Fe_2–$\cdots$ and O_2–Fe_2–$\cdots$) and a ferryl termination are observed for oxidation/reduction cycles in the temperature range from 300 to 823 K with oxygen partial pressures between 10^{-7} mbar and 1 bar (Barbier *et al* 2007). An oxygen termination was also found after annealing at 1100 K and 1 mbar oxygen partial pressure, while annealing at the same temperature and 10^{-5} mbar oxygen partial pressure resulted in a oxygen deficient hydroxylated surface (Ketteler *et al* 2001).

The situation is quite similar for chromia. Theory clearly favors a single chromium termination (Cr–O_3–Cr_2–$\cdots$) at low and intermediate oxygen partial pressures and only at high oxygen pressures is a chromyl ($O{=}Cr$–O_3–Cr_2–$\cdots$) or oxygen (O_3–Cr_2–$\cdots$) termination thought to be stable. The top Cr layer significantly relaxes inward decreasing the interlayer distance between the top Cr layer and the following O_3 layer (Rohrbach *et al* 2004, Rehbein *et al* 1996). For real systems, the presence of superficial defects may enhance the mobility of the surface atoms and an oxygen termination is said to become as likely to occur as a single chromium termination (San Miguel *et al* 1999). Depending on the temperature and the oxygen partial pressure all terminations ranging from the single Cr-terminated (1×1) surface structure over reconstructed and unreconstructed chromyl-terminated structures to the (1×1) O_3-terminated surface structure are found to be theoretically stable configurations (Wang and Smith 2003). The single chromium termination with a large interlayer distance relaxation is found experimentally after sputtering in UHV and annealing in an O_2 atmosphere, flashing the sample up to 1000 K (Rohr *et al* 1997a, 1997b). Termination with a disordered Cr layer including partial occupation of the third octahedral site by chromium between the first and the second O_3 layer was observed after prolonged sputtering and short term annealing at 1200 K in UHV (Gloege *et al* 1999). Preparation at 240 °C and 10^{-5} mbar oxygen partial pressure also led to a single chromium termination (Priyantha and Waddill 2005). To the best of our knowledge, an oxygen-terminated surface has not been reported up to now.

While most experiments were performed with thin films, we analyzed the (0001) surface structures of hematite and chromia bulk single crystals by low energy electron diffraction (LEED). Thereby we avoided structural deviations that might occur in thin films arising from the lattice mismatch between the substrate and the oxide layer. It is interesting to note that in an LEED study of an epitaxial Cr_2O_3 film grown on Cr(110) a $(\sqrt{3} \times \sqrt{3})R30°$ superstructure was observed above 100 K with maximum intensity around 150 K and deceasing intensity above 150 K (Bender *et al* 1995). The superstructure could not be observed at the single crystal surface at temperatures above 120 K. Furthermore, the thin oxide films exhibit two domains as the metal substrates, Pt(111), Ag(111) and Cr(110) have the symmetry $p3m1$ and $pmm2$, while the oxide (0001) surface lacks the mirror plane and has only three-fold symmetry.

As described above, the results of the various investigations are partially contradictory. Theory predominantly predicts similar results for α-Fe_2O_3 and α-Cr_2O_3 including strong interlayer distance relaxations reaching a few layers into the bulk and a single cation termination as the most stable configuration. Therefore we were quite surprised to find out that there are substantial differences between the surface terminations and relaxations of α-$Fe_2O_3(0001)$ and α-$Cr_2O_3(0001)$ bulk single crystals. Although both materials are transition metal oxides with TM^{3+} and crystallize in space group $R\bar{3}c$—and therefore can be expected to be very similar—we found a single cation termination with deep-going relaxations only for α-Fe_2O_3. For α-Cr_2O_3 the two cation positions in the top layer are partially occupied and the interlayer distance relaxation is substantial only for the topmost Cr double layer distance.

2. Experiment

Both crystals were polished and installed in an UHV chamber with a base pressure of 2×10^{-10} mbar. The samples were cut from synthetic crystals. The hematite crystal was annealed at 500 °C in an O_2 atmosphere, $p_{O_2} \approx 3 \times 10^{-8}$ mbar, for several hours. The hematite sample was not sputtered because we wanted to avoid the possible formation of magnetite when annealing the sample above 600 °C. In preliminary experiments we had found by Auger electron spectroscopy (AES) that Ar remained in the surface after sputtering and could only be removed when annealing at higher temperatures. For α-$Cr_2O_3(0001)$ a higher annealing temperature than for α-$Fe_2O_3(0001)$ was necessary to obtain a LEED pattern with reasonably low background. The chromia crystal was sputtered with Ar^+ ions, $E = 1$ keV, $I = 1$–$2\ \mu A\ cm^{-2}$, and afterwards heated up to 900 °C for 5 min under UHV conditions. Both samples showed sharp diffraction spots, although the diffuse background was somewhat elevated for the α-Fe_3O_2 crystal. The LEED patterns of both samples are shown in figure 2.

The LEED patterns exhibit three-fold symmetry as expected for the (0001) surface of space group $R\bar{3}c$. For both samples $I(V)$-curves of 12 symmetrically independent diffraction spots were measured at room temperature. The data were smoothed, the background subtracted and the average over symmetrically equivalent beams was taken. The energy range $E = 150$–500 eV for Fe_2O_3 and 120–550 eV for Cr_2O_3 could be used in the analysis. Charging effects hindered measurements at lower energies as hematite and chromia are insulating oxides with band gaps of 2.1 eV and 4.8 eV,

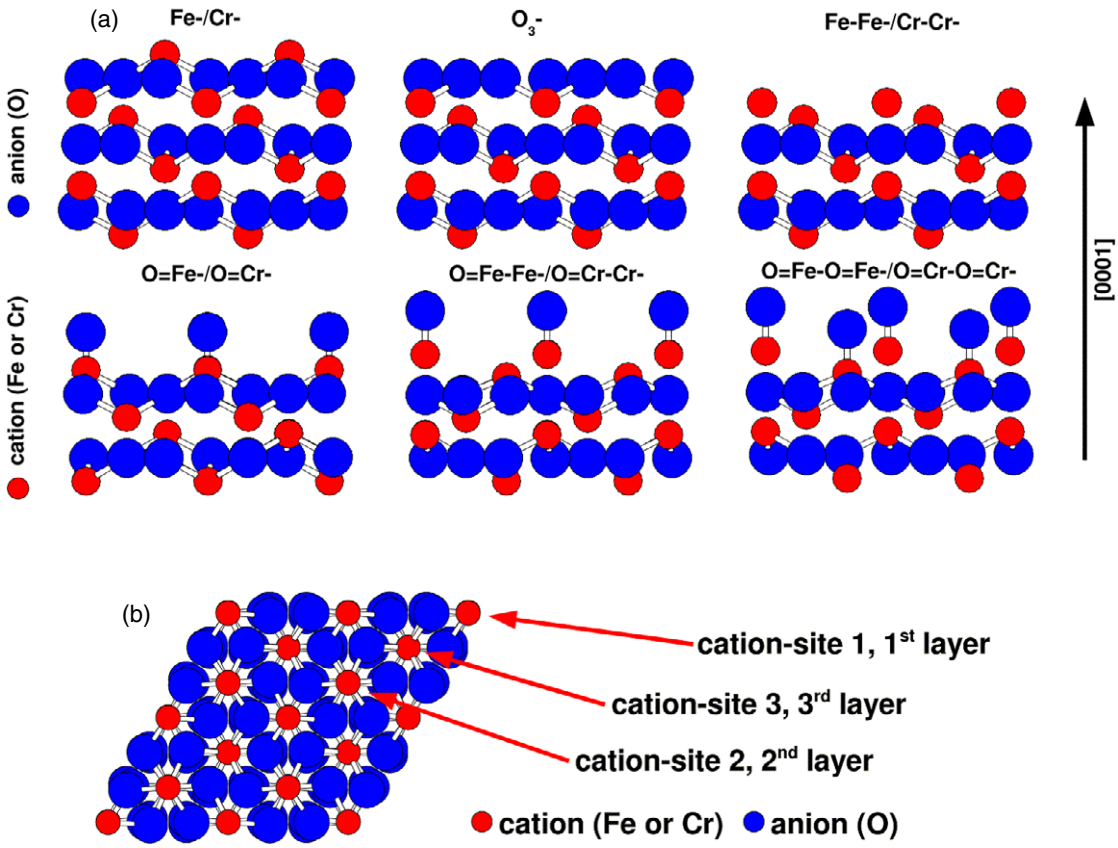

Figure 1. (a) Surface terminations of the corundum-like structure, side view of six different (1 × 1) surface structures. (b) Top view.

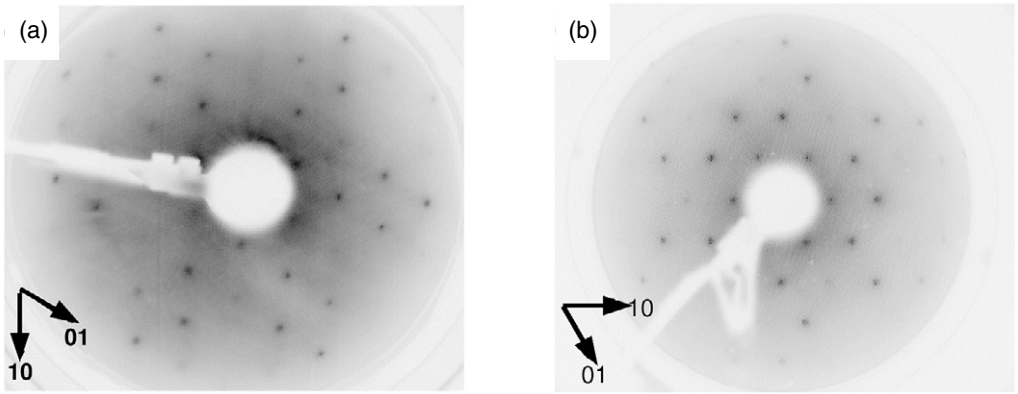

Figure 2. LEED pattern of (a) α-Fe_2O_3 and (b) α-Cr_2O_3 (0001) surfaces. Pictures taken at room temperature, 255 eV and 250 eV, respectively.

respectively. The cleanliness of the surfaces was controlled by AES where no impurities could be detected. In the AES spectra a shift of 5–10 eV to higher energies was observed, which we relate to charging of the sample. The shift disappeared when heating the sample to 300 °C.

3. LEED $I(V)$ analysis

LEED calculations were performed using the layer doubling method and a least squares optimization for refinement of structural and thermal parameters (Over *et al* 1992). The crystal potential was calculated from a superposition of atomic potentials using optimized muffin-tin radii (Rundgren 2003). This method for constructing the muffin-tin potential has been found to compare well to potentials derived from a full DFT calculation and led to reliable results in LEED $I(V)$ analyses for Fe_3O_4(100) (Pentcheva *et al* 2005, 2008) and $Ca_{1.5}Sr_{0.5}TiO_3$ (Nascimento *et al* 2007). Up to 12 phase shifts were used. All possible terminations (see figure 1) and relaxation down to the fourth oxygen layer were optimized. This led to up to 12 positional parameters, the z-coordinates of the top 10 atoms and the x, y position of the

topmost oxygen atom. Lateral shifts in deeper oxygen layers had been considered but were found to be very small and insignificant.

Thermal parameters and occupation factors were optimized for the top four or five atoms, i.e. the top metal layer, the oxygen layer and the next two atoms in the metal layer underneath. Only isotropic displacement parameters, described as Debye temperatures, have been used in the final analysis because calculations with anisotropic parameters did not lead to significant improvement of the fit. Furthermore, it turned out that the agreement in both cases was not good enough to determine a probable enhancement of displacement parameters in the surface layers. Debye temperatures are used to describe isotropic displacements. In the final calculation, therefore, the Debye temperatures were kept fixed at the bulk values. For Fe_2O_3 the bulk values of $\Theta_O = 650$ K and $\Theta_{Fe} = 400$ K were used, derived from neutron diffraction data (Wolska and Schwertmann 1989), and for Cr_2O_3 the values were $\Theta_O = 950$ K and $\Theta_{Cr} = 750$ K derived from x-ray data (Sawada 1994). An optimization of these values has been tried but the misfit of the peaks in some beams for $Cr_2O_3(0001)$ could not be removed. Slightly lower bulk Debye temperatures of 600 and 630 K, as used by Rohr *et al* (1997b) for $Cr_2O_3(0001)$, also did not improve the result. The data set of both samples consisted of 12 symmetrically independent beams with a total energy range of 3950 eV for Cr_2O_3 and 2600 eV for Fe_2O_3. The energy dependence of the real part of the inner potential is approximated by an analytical form $V_0 = A + B/\sqrt{E + C}$ (Rundgren 2003, and further references therein) where A, B and C are parameters depending on the chemical composition, the structure and the muffin-tin radii, and E is the energy of the primary beam in eV. The parameters of the energy dependency are calculated in the phase shift program (Rundgren 2003) and have been kept fixed in the LEED analysis where only the constant A has been optimized to take account of the muffin-tin zero, experimental errors and the work function difference between the electron gun and the sample. For Fe_2O_3 we used $V_0(E) = -86.8/\sqrt{E + 4.8}$, and for Cr_2O_3 we used $V_0(E) = -86/\sqrt{E + 4.0}$.

3.1. Results for α-Fe$_2$O$_3$(0001)

The comparison of the $I(V)$-curves for the best fit model is shown in figure 3; the R-factor is $R_P = 0.34$. Pendry's R-factor has been used (Pendry 1980). The agreement is not quite satisfactory but is comparable to that found in other LEED analyses of oxide surfaces. The structural results and the comparison with previous theoretical and experimental results are shown in tables 1 and 2. Our results agree qualitatively with the DFT calculations and indicate that the α-$Fe_2O_3(0001)$ surface is terminated by a single iron, i.e. the (Fe–O_3–Fe_2–O_3–$\cdots$) termination (see figure 4). The surface exhibits considerable disorder, the top Fe position is only half occupied and vacancies exist in the top oxygen layer as well as in the Fe positions below the top oxygen layer. The oxygen positions were allowed to vary in the top three oxygen layers, but only in the top layer was a small shift determined—in the deeper layers the oxygen atoms remain in the bulk position. The oxygen

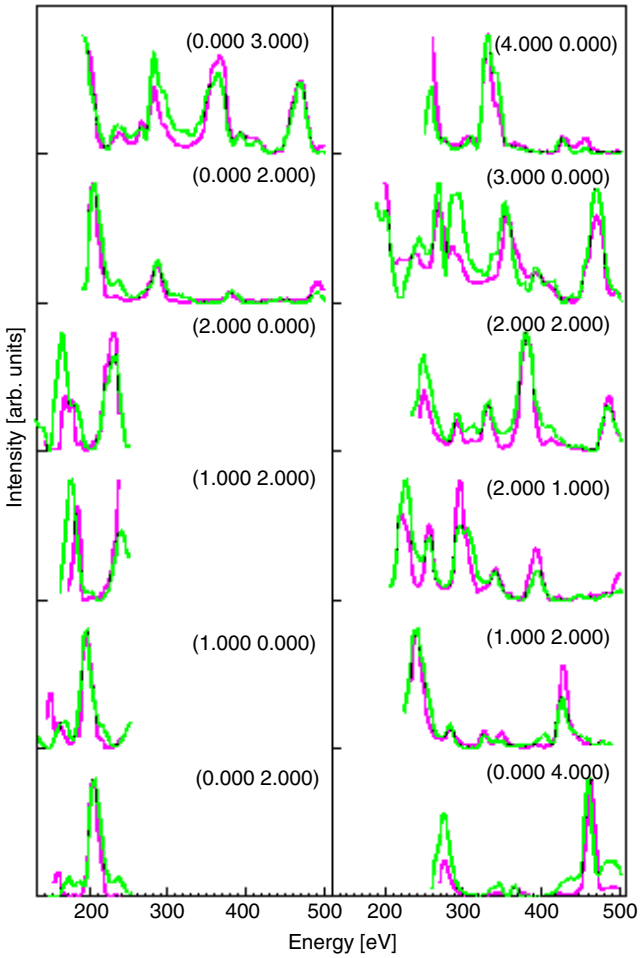

Figure 3. Best fit calculated $I(V)$-curves for α-$Fe_2O_3(0001)$ (green/light grey line) compared to experimental curves (magenta/black line).

distances in the top layer are between 2.6 and 3.17 Å and very close to the bulk values between 2.67 and 3.03 Å. The Fe–O bond length of the top Fe is 1.86 Å, slightly smaller than in the bulk, and in the second layer the two bond lengths are 2.02 and 2.05 Å; the bulk values are 1.94 and 2.11 Å.

It is interesting to note that partial occupation of the top Fe layer was also reported in the DFT study of Rohrbach *et al* (2004). Partial occupation therefore is probably not related to the preparation conditions. The remaining misfit in the $I(V)$ analysis may result from the insulating crystal and from defects occurring during annealing in oxygen-poor conditions. Charging of the sample probably causes a shift of the peak positions which is energy dependent and which is not reproduced by the energy dependence of the inner potential. The marginal agreement leaves large uncertainties in the structural parameters and occupation factors. Nevertheless, the (Fe–O_3–Fe_2–$O_3\cdots$) termination and the partial occupation of the top Fe position can be safely concluded, as all models with different terminations and full occupation of all sites resulted in a significantly larger R-factor $R_P > 0.58$.

Comparing the results to the DFT calculations the main difference is found in the relaxation of the top layer distance. Our LEED analysis finds a value of -27%, significantly less

Table 1. Coordinates and occupation factors of the most likely model. The lattice constants used in the calculations are $a = 5.035$ Å, $c = 13.746$ Å. The asterisk indicates fixed parameters.

	Bulk			LEED			
Atom	Z (Å)	X (rel. units)	Y (rel. units)	Z (Å)	X (rel. units)	Y (rel. units)	Occ. (%)
Fe(1)	0.6	0.33	−0.33	0.85	0.333*	−0.333*	51
O(1)	1.45	0.3606	0.3333	1.47	0.377	0.349	92
Fe(2)	2.29	0.0	0.0	2.34	0.00*	0.00*	70
Fe(3)	2.88	−0.333	0.333	2.89	−0.333*	0.333*	98
O(2)	3.72	0.306	0.00	3.79	0.306	0.00	100*
Fe(4)	4.58	0.333	−0.333	4.62	0.333*	−0.333*	100*
Fe(5)	5.18	0.0	0.00	5.25	0.000*	0.000*	100*
O(3)	6.02	0.027	−0.330	6.06	0.027	−0.333	100*
Fe(6)	6.87	−0.333	0.333	6.90	−0.333*	0.333*	100*
Fe(7)	7.47	0.333	−0.333	7.52	0.333*	−0.333*	100*
O(4)	8.32*	−0.027	0.333	8.32*	−0.027*	0.333*	100*

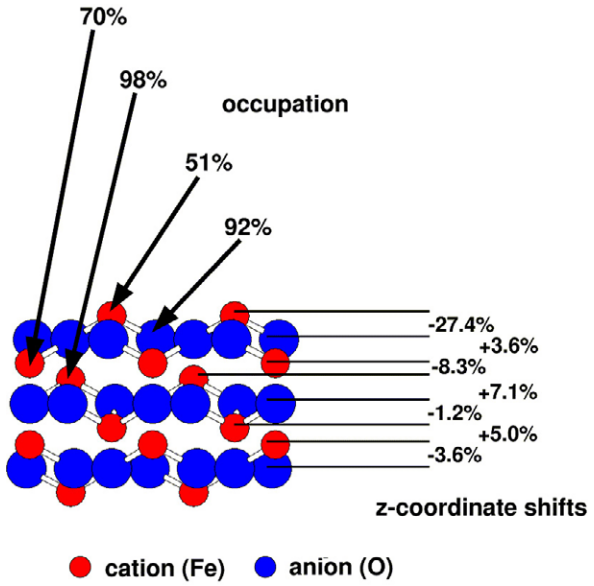

Figure 4. The most likely model for α-Fe_2O_3(0001) surface termination with z-coordinate shifts and occupation.

Table 2. Comparison of the results of this study with previous results from DFT calculations, one previous LEED study and an XPD study. The layer distances in the bulk are Fe–O = 0.844 Å, and Fe–Fe = 0.6 Å.

	This study	DFT[a]	DFT[b]	LEED[c]	XPD[d]
Atom	ΔZ (%)	ΔZ (%)	ΔZ (%)	ΔZ (%)	ΔZ (%)
Fe(1)–O(1)	−27.4	−57	−51.3	−79	−41
O(1)–Fe(2)	3.6	9.6	6.4	4.0	18
Fe(2)–Fe(3)	−8.3	−4	−31.7	35	−8
Fe(3)–O(2)	7.1	13	13.1	−28	47
O(2)–Fe(4)	−1.2	3.5	0.1		
Fe(4)–Fe(5)	5	−3			
Fe(5)–O(3)	−3.6				
O(3)–Fe(6)	0				
Fe(6)–Fe(7)	0				
Fe(7)–O(4)	0				
O(4)	Fixed				

[a] Rohrbach *et al* (2004).
[b] Bergermayer *et al* (2004).
[c] Ketteler *et al* (2001).
[d] Thevuthasan *et al* (1999).

than found in the DFT calculations where −51% and −57% have been determined (Rohrbach *et al* 2004, Bergermayer *et al* 2004). The differences in deeper layers are certainly within the error limits, which may be estimated to about 5%. The DFT calculations for the surface structure under UHV conditions therefore agree qualitatively with the LEED results. Larger differences are found with the results of the previous LEED study by Ketteler *et al* (2001). There, a much larger relaxation was found. It has to be mentioned that Ketteler *et al* (2001) found better agreement for an oxygen-terminated than for an iron-terminated surface with a lower R-factor of $R_P = 0.227$. In this study a smaller data set was used in the lower energy range and the data are therefore not directly comparable to those measured here. The different results may be related to the different preparation methods. Ketteler *et al* (2001) grew a magnetite thin film on Pt(111) which was then annealed in 10^{-5} mbar oxygen pressure and converted to hematite, while the specimen we used was annealed in 3×10^{-8} mbar oxygen atmosphere. This might be the reason why Ketteler *et al* found an oxygen-terminated surface. Strain effects do not seem to be a very likely explanation for the discrepancy as they analyzed films with a thickness of several tens of nanometers. Nevertheless, the lattice mismatch between the Pt(111) substrate and the Fe_2O_3(0001) thin film can introduce slight lattice distortions in the hematite which then do not fully relax to bulk values even at some 10 nm thickness.

Comparing the present results to an XPD study by Thevuthasan *et al* (1999) performed on a hematite thin film grown on Al_2O_3(0001) we again find smaller interlayer relaxations, especially for the first two interlayers. Lemire *et al* (2005) prepared hematite thin films on Pt(111) in considerably higher oxygen partial pressures than those in which we prepared our α-Fe_2O_3(0001) single crystal surface. They found ferryl groups (O=Fe-groups) coexisting with a Fe termination. Our oxygen-poor preparation conditions hinder the formation of ferryl groups and we only observed the Fe termination.

Table 3. Coordinates of the most likely model for $Cr_2O_3(0001)$. The z-coordinates and occupation factors of O(1) and O(2) refer to the model with partial chromyl termination. The occupation of O(1) and (2) positions has a negligible influence on the other parameters. The x, y coordinates of the oxygen atoms remain at the bulk positions. The asterisk indicates fixed z-coordinates.

		Bulk	LEED
Atom	Z (Å)	Z (Å)	occ. (%)
Oad(2)		−2.0	24
Cr(2)	0.0	0.0	31
Oad(1)		−1.73	26
Cr(1)	0.38	0.27	61
O(1)	1.32	1.31	80
Cr(3)	2.26	2.27	48
Cr(4)	2.64	2.65	54
O(2)	3.58	3.58*	100*
Cr(5)	4.52	4.52*	
Cr(6)	4.90	4.90*	
O(3)	5.84	5.84*	

Table 4. Comparison of the relaxation of layer distances to DFT results, an earlier LEED analysis and a surface XRD (SXRD) analysis. Δz is the relaxation compared to the bulk value, Cr–Cr = 0.38 Å and Cr–O = 0.94 Å.

	LEED	DFT[a]	LEED[b]	SXRD[c]
Atom	ΔZ (%)	ΔZ (%)	ΔZ (%)	ΔZ (%)
Oad(2)–Cr(2)				
Cr(2)–Cr(1)	−28.9			
Oad(1)–Cr(1)				
Cr(1)–O(1)	10.6	−60	−60	−6
O(1)–Cr(3)	2.1	12	−3	0
Cr(3)–Cr(4)	0.0	−44	−21	−26
Cr(4)–O(2)	1.1	9.2	6	7
O(2)–Cr(5)	0			
Cr(5)–Cr(6)	0			
Cr(6)–O(3)	Fixed			
O(3)–Cr(7)	Fixed			

[a] Rohrbach *et al* (2004).
[b] Rohr *et al* (1997b).
[c] Gloege *et al* (1999).

3.2. Results for α-$Cr_2O_3(0001)$

Only poor agreement could be achieved for the α-$Cr_2O_3(0001)$ surface. The 'best fit' R-factor is $R_P = 0.48$. The comparison between experimental and calculated $I(V)$-curves is shown in figure 5. The model is the (Cr–Cr–O_3–Cr_2–···) termination with partial occupation of the two Cr sites in the top layer. It cannot be decided on the basis of the present LEED results whether the surface is terminated by chromyl groups or metal atoms. Similar agreement with only a slightly worse R-factor, $R_P = 0.50$, was obtained for the chromyl termination (O=Cr–O=Cr–O_3–Cr_2–···; see figure 6). The results for both models show partial occupation of the two top Cr positions or chromyl groups, respectively. The additional oxygen present in the chromyl termination had no significant influence on the structural parameters, neither coordinates nor occupation. The structural results and the comparison with previous results are given in tables 3 and 4. The surface is considerably disordered, which is consistent with the enhanced background

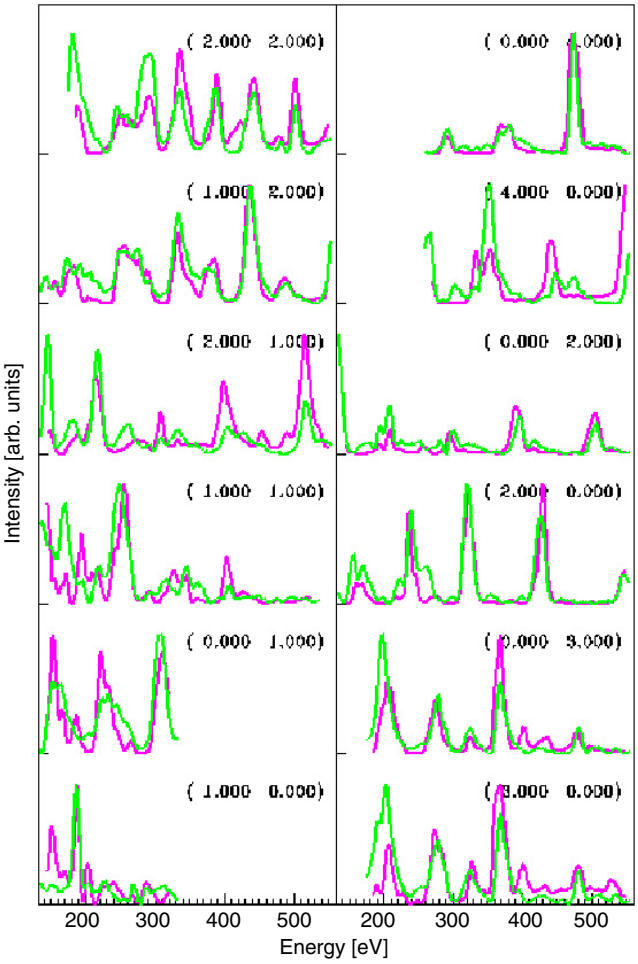

Figure 5. Best fit calculated $I(V)$-curves for α-$Cr_2O_3(0001)$ (green line) compared to experimental curves (magenta line).

intensity visible in figure 2. The top oxygen layer exhibits 20% vacancies and the second Cr double layer is also only half occupied. We present this result in spite of the insufficient agreement because all other terminations, i.e. the single Cr termination analogous to the $Fe_2O_3(0001)$ surface, led to an R-factor of $R_P > 0.65$. The model with partial occupation of both Cr sites reproduces qualitatively the main peak positions and intensities of the experimental curves. This is not the case for all other models. Another argument supporting this model is a good agreement with an x-ray study of the same surface. In an independent x-ray study using the same preparation conditions for the clean α-$Cr_2O_3(0001)$ surface very similar structural results and disorder were found, in particular the partial occupation of both Cr sites in the first and second Cr double layer and small relaxation in the deeper layers. The x-ray result favors the chromyl termination. The results of this study will be published in a separate paper together with the results from measurements at higher oxygen pressures (Bikondoa *et al* 2009). The relaxation in deeper layers is small and the atoms remain nearly in bulk positions. The agreement is marginal, but significantly worse for other models.

In our LEED study we cannot distinguish between the Cr–Cr– and the O=Cr–O=Cr termination, but the chromyl termination seems to be unlikely from theoretical predictions

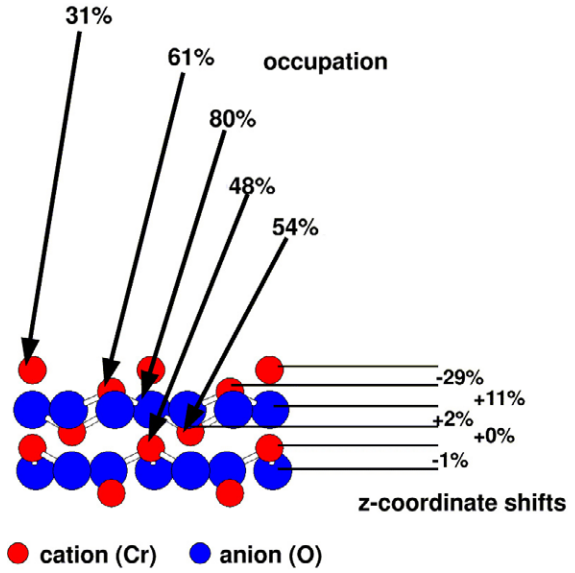

Figure 6. The most likely model for α-Cr_2O_3(0001), surface termination with z-coordinate shifts and occupation.

and from the preparation conditions in UHV. On the other hand, the small relaxation in deeper layers and the expansion of the normal distance Cr(1)–O(1) not found in the theoretical study supports the chromyl termination. The structure differs from that predicted by DFT calculations as well as from the previous LEED results (Rohr *et al* 1997a, 1997b). Both find a Cr termination with strong interlayer contraction of the topmost Cr–O distance. This interlayer distance is expanded in our results but one has to keep in mind that we found two partially occupied Cr positions in the top layer. The discrepancy may have its origin in the different samples. We have investigated the surface of a bulk crystal, while in the previous LEED study an epitaxial film grown on Cr(110) was investigated. The lattice mismatch to the substrate can be considered as a possible source for the discrepancy since a film only a few nanometers thick was investigated, but it seems more likely that the different preparation conditions are responsible for the different structural results. The surface here was sputtered and annealed in UHV and the surface exhibits a considerable amount of disorder.

The only other experimental study on a Cr_2O_3(0001) surface was the x-ray study by Gloege *et al* (1999) which was also done with the same bulk crystal and came to different results. Gloege *et al* (1999) found a Cr termination but with a partially occupied Cr interstitial position below the topmost oxygen layer. The topmost Cr–O interlayer distance is reported to be only slightly contracted (-6%). This result could not be reproduced in the present LEED analysis. All models with occupation of an interstitial site led to R-factors >0.8 and a fit of the data always removed the interstitial atom. Since the surface was prepared in the same way the discrepancy must have its origin in the data sets or in the analysis. In our LEED study we used a large data set but could not achieve sufficient agreement. We relate this to surface disorder and possible errors in the data due to sample charging by the LEED beam. Nevertheless, in spite of the large R-factor we conclude that a partial occupation of the interstitial site can be excluded. In the x-ray study by Gloege *et al* (1999) the best agreement was found for the interstitial model, but the model with a single Cr in the top layer was the second best model. A model with partial occupation of the two Cr positions in the top layer has not been investigated. The data set which could be measured in the x-ray study is probably too small. In a new x-ray study with a larger data set (Bikondoa *et al* 2009) the interstitial site was not found.

4. Summary

The LEED $I(V)$ analyses for clean α-Fe_2O_3(0001) and α-Cr_2O_3(0001) surfaces under UHV conditions show marked differences. For α-Fe_2O_3(0001) the result supports the predictions from DFT calculations, i.e. single Fe termination and relaxation in deeper layers, where the vertical distance between the Fe positions is lowered and the oxygens remain nearly in bulk positions. The main discrepancy with the DFT results occurs in the relaxation of the top Fe towards the oxygen layer, which is about half of the predicted value. The partial occupation of the top Fe is consistent with the DFT calculations and the observation of a high background in the LEED pattern. A markedly different surface structure is found for α-Cr_2O_3(0001). The results differ from that predicted by DFT calculations; the best agreement is obtained for the (Cr–Cr–O_3–Cr_2–$\cdots$) termination where both Cr sites are partially occupied. The partial occupation with chromyl, i.e. (O=Cr–O=Cr–O_3–Cr–Cr–O_3–$\cdots$) termination, leads to similar agreement and cannot be excluded in the present analysis. Relaxations in deeper layers are small and the atoms below the top oxygen layer remain nearly in bulk positions. The agreement in the LEED $I(V)$ analysis is clearly not sufficient to determine the structure unambiguously, and our conclusions are based on the exclusion of all other models. The remaining misfit may also be caused by the insulating character of the oxide crystals, which may cause defects induced by the electron beam.

Acknowledgments

We gratefully acknowledge funding by the DFG grant no. Pe883/4-1 and ESF within the European Mineral Science Initiative EuroMinSci.

References

Barbier A, Stierle A, Kasper N, Guittet M-J and Jupille J 2007 *Phys. Rev.* B **75** 233406
Bender M, Ehrlich D, Yakovkin I N, Rohr F, Bäumer M, Kuhlenbeck H, Freund H-J and Staemmler V 1995 *J. Phys.: Condens. Matter* **7** 5289–301
Bergermayer W, Schweiger H and Wimmer E 2004 *Phys. Rev.* B **69** 195409
Bikondoa O, Lindsay R, Kim H, Moritz W and Thornton G 2009 in preparation
Chambers S A 2006 *Surf. Sci. Rep.* **61** 345–81
Chambers S A and Yi S I 1999 *Surf. Sci.* **439** L785–91
Gloege Th, Meyerheim H L, Moritz W and Wolf D 1999 *Surf. Sci.* **441** L917–23

Ketteler G, Weiss W and Ranke W 2001 *Surf. Rev. Lett.* **8** 661–83
Lemire C, Bertarione S, Zecchina A, Scarano D, Chaka A M, Shaikhutdinov Sh K and Freund H-J 2005 *Phys. Rev. Lett.* **94** 166101
Nascimento V B, Moore R G, Rundgren J, Zhang J, Cai L, Jin R, Mandrus D G and Plummer E W 2007 *Phys. Rev.* B **75** 035408
Over H, Ketterl U, Moritz W and Ertl G 1992 *Phys. Rev.* B **46** 15438–46
Pendry J B 1980 *J. Phys. C: Solid State Phys.* **13** 937
Pentcheva R, Moritz W, Rundgren J, Frank S, Schrupp D and Scheffler M 2008 *Surf. Sci.* **602** 1299–305
Pentcheva R, Wendler F, Meyerheim H L, Moritz W, Jedrecy N and Scheffler M 2005 *Phys. Rev. Lett.* **94** 126101
Priyantha W A A and Waddill G D 2005 *Surf. Sci.* **578** 149–61
Rehbein C, Harrison N M and Wander A 1996 *Phys. Rev.* B **54** 14066–70
Rohr F, Bäumer M, Freund H-J, Mejias J A, Staemmler V, Müller S, Hammer L and Heinz K 1997a *Surf. Sci.* **372** L291–7
Rohr F, Bäumer M, Freund H-J, Mejias J A, Staemmler V, Müller S, Hammer L and Heinz K 1997b *Surf. Sci.* **389** 391
Rohrbach A, Hafner J and Kresse G 2004 *Phys. Rev.* B **70** 125426
Rundgren J 2003 *Phys. Rev.* B **68** 125405
San Miguel M A, Álvarez L J, Fernández Sanz J and Odriozola J A 1999 *J. Mol. Struct. (Theochem)* **463** 185–90
Sawada H 1994 *Mater. Res. Bull.* **29** 239–45
Shaikhutdinov Sh K and Weiss W 1999 *Surf. Sci.* **432** L627–34
Thevuthasan S, Kim Y J, Yi S I, Chambers S A, Morais J, Denecke R, Fadley C S, Liu P, Kendelewicz T and Brown G E Jr 1999 *Surf. Sci.* **425** 276–86
Trainor T P, Chaka A M, Eng P J, Newville M, Waychunas G A, Catalano J G and Brown G E Jr 2004 *Surf. Sci.* **573** 204–24
Wang X-G and Smith J R 2003 *Phys. Rev.* B **68** 201402(R)
Wang X-G, Weiss W, Shaikhutdinov Sh K, Ritter M, Petersen M, Wagner F, Schlögl R and Scheffler M 1998 *Phys. Rev. Lett.* **81** 1038–41
Wolska E and Schwertmann U 1989 *Z. Kristallogr.* **189** 223–37